Journal of Luminescence 197 (2018) 169–174

Contents lists available at ScienceDirect

Journal of Luminescence

journal homepage: www.elsevier.com/locate/jlumin

Photoluminescence properties of red-emitting $Li_2ZnSn_2O_6:Mn^{4+}$ phosphor for solid-state lighting

Renping Cao[a,*], Xing Liu[a], Kailei Bai[a], Ting Chen[a], Siling Guo[a], Zuofu Hu[a], Fen Xiao[b], Zhiyang Luo[b]

[a] College of Mathematics and Physics, Jinggangshan University, Ji'an 343009, China
[b] College of Mechanical Manufacture and Automation, Jinggangshan University, Ji'an 343009, China

ARTICLE INFO

Keywords:
Stannate
Phosphor
Mn^{4+} ion
Deep-red emitting

ABSTRACT

Novel $Li_2ZnSn_2O_6:Mn^{4+}$ (LZSO:Mn^{4+}) phosphor is prepared by the high temperature solid-state reaction method in air. The X-ray powder diffractions of samples with a hexagonal LZSO crystal system are investigated. Excitation spectrum of LZSO:Mn^{4+} phosphor monitored at 658 nm shows these excitation bands in the range of 220 − 570 nm, which are attributed to the Mn^{4+} - O^{2-} charge transfer band (220 − 300 nm), the $^4A_2 \rightarrow {}^4T_1$ transition of Mn^{4+} ion (300 − 420 nm), and $^4A_2 \rightarrow {}^4T_2$ transition of Mn^{4+} ion (420 − 570 nm), respectively. LZSO:Mn^{4+} phosphor with excitation at 335 and 480 nm emits deep-red light with the strongest emission peak at ~ 658 nm in the range of 600 − 780 nm due to the $^2E \rightarrow {}^4A_2$ transition of Mn^{4+} ion. The optimal Mn^{4+} concentration is ~ 0.4% in LZSO:Mn^{4+} phosphor. The lifetime of LZSO:Mn^{4+} phosphor decreases from 14.32 to 12.05 μs with increasing Mn^{4+} concentration from 0.2% to 1.0%. The luminous mechanism and energy level splitting of Mn^{4+} ion in LZSO:Mn^{4+} phosphor are explained by the Tanabe-Sugano energy level diagram.

1. Introduction

Among many transition metal ions (e.g., Cr^{3+}, Cu^{2+}, Fe^{3+}, Mn^{2+}, Ti^{4+}, Mn^{4+} etc), Mn^{4+} ion is attracting increasing attention and widely used in the design of red-emitting phosphors, which is identified as an alternative to rare earth ions for the fabrication of suitable phosphors [1–3]. Mn^{4+} ion has $3d^3$ electron configuration with the incompletely filled shell and usually locates in the octahedral sites of solids and its energy level splitting may be explained by the Tanabe–Sugano diagram [4]. Mn^{4+} ion is a suitable activator for red phosphor and Mn^{4+}-doped luminescent materials usually show both broad excitation band covering from 200 to 550 nm due to the $^4A_2 \rightarrow ({}^4T_1, {}^2T_2$, and $^4T_2)$ transitions and red to near-infrared emission in the region from 620 to 780 nm owing to the $^2E \rightarrow {}^4A_2$ transition [5]. The luminescence properties of Mn^{4+} ion can usually rely heavily on the crystal field of host.

Since the synthesis of Mn^{4+}-doped luminescent materials was reported in 1947 [6], the research on this topic is attracting a range of interest. Mn^{4+} ion can usually be doped into the hosts with octahedral coordination, which are mainly divided into two categories: fluorides and oxides. In fluoride hosts, Mn^{4+} ion exhibits broad excitation band with the most intense peak at ~ 460 nm and very sharp emission lines peaking at ~ 630 nm. Some examples of such phosphors are $R_2MF_6:Mn^{4+}$ (R = Li, Na, K, Rb, Cs; M = Ti, Si, Ge, Zr, Sn), $ZnTiF_6{\cdot}6H_2O:Mn^{4+}$, $BaSnF_6:Mn^{4+}$, $BaSiF_6:Mn^{4+}$, $BaTiF_6:Mn^{4+}$, $Na_3TaF_8:Mn^{4+}$, $K_3AlF_6:Mn^{4+}$, $K_3ZrF_7:Mn^{4+}$, $KNaSiF_6:Mn^{4+}$, $(NH_4)_2TiF_6:Mn^{4+}$, $K_2LiAlF_6:Mn^{4+}$, and $K_2LiGaF_6:Mn^{4+}$ [7–29]. In oxide hosts, the most intense excitation peak of Mn^{4+} usually appears in the range of 289 − 350 nm and the emission peak position can be observed over a wide range from red (> 640 nm) to near-infrared (< 730 nm) region. They are (1) Mn^{4+}-doped germanates ($Ba_2GeO_4:Mn^{4+}$, $Li_3RbGe_8O_{18}:Mn^{4+}$, $Li_2MgGeO_4:Mn^{4+}$, $Li_2GaGe_2O_6$, $SrGe_4O_9:Mn^{4+}$, $K_2Ge_4O_9:Mn^{4+}$, $Mg_{3.5}Ge_{1.25}O_6:Mn^{4+}$, $Mg_3Ga_2GeO_8:Mn^{4+}$, $K_2BaGe_8O_{18}:Mn^{4+}$, $LiNaGe_4O_9:Mn^{4+}$, $Mg_7Ga_2GeO_{12}:Mn^{4+}$, $Ba_2TiGe_2O_8:Mn^{4+}$, and $La_3GaGe_5O_{16}:Mn^{4+}$) [30–42], (2) Mn^{4+}-doped gallates ($LiGa_5O_8:Mn^{4+}$, $ZnGa_2O_4:Mn^{4+}$, $Gd_3Ga_5O_{12}:Mn^{4+}$, and $LaGaO_3:Mn^{4+}$) [43–46], (3) Mn^{4+}-doped aluminates ($CaAl_{12}O_{19}:Mn^{4+}$, $Sr_2MgAl_{22}O_{36}:Mn^{4+}$, $CaAl_2O_4:Mn^{4+}$, $SrAl_4O_7:Mn^{4+}$, $Sr_4Al_{14}O_{25}:Mn^{4+}$, $CaMg_2Al_{16}O_{27}:Mn^{4+}$, $Ca_{14}Zn_6Al_{10}O_{35}$, $CaYAlO_4:Mn^{4+}$, $Na_2MgAl_{10}O_{17}:Mn^{4+}$) [47–55], (4) Mn^{4+}-doped titanates ($Li_2TiO_3:Mn^{4+}$, $BaTiO_3:Mn^{4+}$, $Gd_2MgTiO_6:Mn^{4+}$, $Li_2MgTiO_4:Mn^{4+}$, $La_2MgTiO_6:Mn^{4+}$, $LiGaTiO_4:Mn^{4+}$, $SrTiO_3:Mn^{4+}$, $Y_2Ti_2O_7:Mn^{4+}$, $Mg_2TiO_4:Mn^{4+}$, $BaMg_6Ti_6O_{19}:Mn^{4+}$, and $Mg_2Ge_xTi_{1-x}O_4:Mn^{4+}$) [56–66], (5) Mn^{4+}-doped zirconates ($CaZrO_3:Mn^{4+}$ and $Li_2MgZrO_4:Mn^{4+}$) [67,68], (6) Mn^{4+}-doped niobate ($Li_3Mg_2NbO_6:Mn^{4+}$, $Ba_2LaNbO_6:Mn^{4+}$, and $Ba_2GdNbO_6:Mn^{4+}$) [69–71], (7) Mn^{4+}-doped other oxides ($MgAl_2Si_2O_8:Mn^{4+}$, $Li_2Mg_3SnO_6:Mn^{4+}$, $NaLaMgTeO_6:Mn^{4+}$,

---

[*] Corresponding author.
E-mail address: jxcrp@163.com (R. Cao).

https://doi.org/10.1016/j.jlumin.2018.01.023
Received 26 November 2017; Received in revised form 4 January 2018; Accepted 13 January 2018

$Ca_3Al_4ZnO_{10}$:Mn^{4+}, La_2LiTaO_6:Mn^{4+}, Sr_2ZnWO_6:Mn^{4+}, and $Ca_{14}Zn_6Ga_{10}O_{35}$:Mn^{4+}) [72–78]. In addition, nitrides used as the host of Mn^{4+} have also been reported (such as AlN:Mn^{4+} and GaN:Mn^{4+}) [79,80].

There are differences in the excitation and emission peak positions of different Mn^{4+}-doped luminescent materials. The covalency and coordination symmetry of the "Mn^{4+} - ligand" bonding have a large effect on the red-emitting wavelengths including several associated vibronic sidebands because of the spin-forbidden transition ^2E - $^4A_2$ of Mn^{4+} [81]. Therefore, the host lattice plays an important role in the optical properties of Mn^{4+}-doped luminescent materials. The complex oxide $Li_2ZnSn_2O_6$ (LZSO) has good physical properties (good stabilization, electronic and ionic transport, reversible lithium intercalation, electrochemical sensing, etc) and is few used as host of phosphor. $Li_2ZnSn_2O_6$ contains [SnO_6] octahedron, which makes the Mn^{4+} ion to be replaced by Sn^{4+} ion [82]. Up to now, $Li_2ZnSn_2O_6$:Mn^{4+} (LZSO:Mn^{4+}) phosphor is rarely reported. Thus this phosphor is selected here as the research object for examining the basic luminescence properties of Mn^{4+} ion in oxide host.

In this work, a series of LZSO:Mn^{4+} phosphors are prepared by the high temperature solid-state reaction method in air. We investigate the crystal structure, morphology, luminescence properties, lifetime, and quantum efficiency (QE) of phosphors. The influences of Mn^{4+} concentration to luminescence properties and lifetimes are discussed. The luminous mechanism is explained by the Tanabe-Sugano energy level diagram.

2. Experimental section

2.1. Raw materials and furnace

We use pure Li_2CO_3 (99.5%), ZnO (99.9%), SnO_2 (99.9%), and $MnCO_3$ (99.5%) as raw materials in this work, which are purchased from the Aladdin Chemical Reagent Company in Shanghai, China. These raw materials are further unpurified. The rectangular aluminum oxide ark and cylindrical aluminum oxide crucible (~ 5 ml) are used as furnace for sintering.

2.2. Synthetic process

$Li_2ZnSn_{(2-x)}O_6$:xMn^{4+} (LZSO:xMn^{4+}) (x = 0, 0.2, 0.4, 0.6, 0.8, and 1.0 mol%) phosphors are prepared by using the conventional solid-state reaction method in air. According to the stoichiometric composition, the raw materials are weighed and ground thoroughly for 20 min in an agate mortar and sintered in a furnace at 650 °C for 6 h in air. After cooled down to the room temperature, the mixture is reground thoroughly for 20 min. Then the mixture is sintered again at 1150 °C for 5 h in air.

2.3. Properties characterization

Here, we use X-ray powder diffraction (XRD) diffractometer (Philips Model PW1830) with a graphite monochromator to measure the crystalline phases of all phosphors. Cu-Kα is used as irradiation source with 40 kV and 40 mA. We collect the XRD pattern data with a step scanning rate of 0.02° in the 2θ range of 10 − 90° at room temperature. We observe the size and morphology of the phosphor using a (Phenom Prox) scanning electron microscopy (SEM) with 15 kV.

We investigate luminescence properties and decay curves of the phosphors by a steady-state FLS980 spectrofluorimeter (Edinburgh Instruments, UK, Edinburgh) with a high spectral resolution ratio (signal to noise ratio > 12000:1). The excitation source for steady-state spectrum measurement is a 450 W ozone free xenon lamp. A microsecond pulsed xenon flash lamp µF900 with an average power of 60 W is available to record the decay curves for lifetimes. The QE is measured directly by the steady-state FLS980 spectrofluorimeter with an integrating sphere.

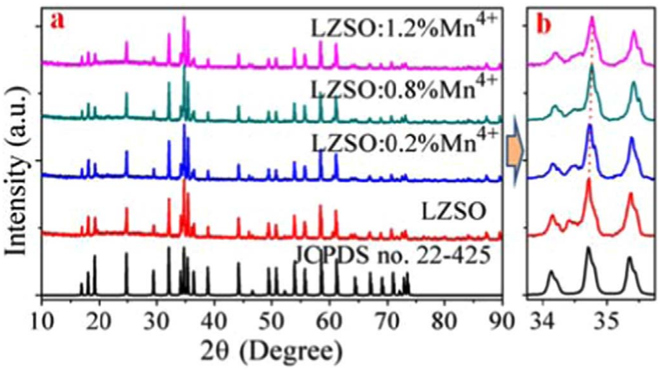

Fig. 1. (a) XRD patterns of JCPDS no. 22–425 (LZSO), LZSO:xMn^{4+} (x = 0, 0.2%, 0.8%, and 1.2%) phosphors at room temperature, (b) XRD patterns in the range of 33.75 − 35.75°.

3. Results and discussion

XRD patterns of LZSO:xMn^{4+} (x = 0, 0.2%, 0.8%, and 1.2%) phosphors at room temperature are collected to verify the phase purity. As is shown in Fig. 1(a), it can be seen clearly that XRD patterns of samples follow well with that of the Joint Committee on Powder Diffraction Standards (JCPDS) no. 22–425 (LZSO), suggesting that LZSO:Mn^{4+} with different Mn^{4+} concentration are synthesized in a single phase structure and that Mn^{4+} ion is doped into the host crystal lattice instead of forming impurity phases. The host LZSO belongs to a hexagonal crystal system and its lattice parameters are a = 6.05 Å and c = 9.86 Å [82]. In host LZSO lattice, Mn^{4+} ion replaces Sn^{4+} ion in [SnO_6] octahedron. Since the ionic radius of Mn^{4+} ion (~ 0.54 Å, six-coordinated) is smaller than that of Sn^{4+} ion (~ 0.69 Å, six-coordinated) [83], these peaks of XRD pattern have a bit red shift with increasing Mn^{4+} ion content as the amount of Sn^{4+} ions are replaced by Mn^{4+} ions, which is shown in Fig. 1(b). Each peak can be well explained by the Bragg Eq. ($2d \sin\theta = n\lambda$, where d is the spacing between the planes in the atomic lattice, λ is the wavelength of the X-ray, and θ is diffraction angle between the incident ray) [84].

The SEM image of LZSO:0.4%Mn^{4+} phosphor at room temperature is shown in Fig. 2. The LZSO:0.4%Mn^{4+} phosphor has approximate spherical morphology, which is assistance for the application of phosphors in solid-state lighting, and its size is in the range of 0.6 µm − 1.5 µm.

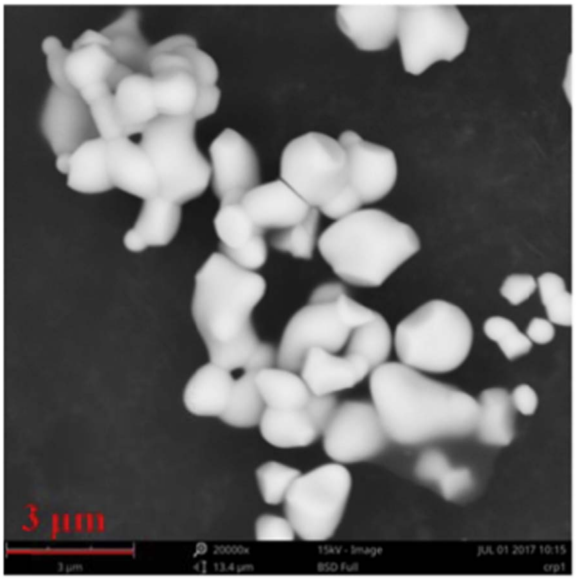

Fig. 2. SEM image of LZSO:0.4%Mn^{4+} phosphor at room temperature.